Available online at www.sciencedirect.com

ScienceDirect

Advances in Space Research 67 (2021) 3744–3754

ADVANCES IN SPACE RESEARCH (a COSPAR publication)

www.elsevier.com/locate/asr

Orbit insertion error analysis for a space-based gravitational wave observatory

Zhuo Li *, Jianhua Zheng, Mingtao Li

National Space Science Center, Chinese Academy of Sciences, Beijing 100190, China
University of Chinese Academy of Sciences, Beijing 100039, China

Received 31 December 2019; received in revised form 12 December 2020; accepted 17 December 2020
Available online 29 December 2020

Abstract

Constellation is required to be highly stable over several years for a space-based gravitational wave observatory. However, the stability of the constellation can be affected by orbit insertion errors. The effects of orbit insertion errors on the constellation are mainly studied in this paper. Firstly, Monte-Carlo, Unscented Transformation Covariance Analysis Method (UTCAM) and Spherical Simplex Unscented Transformation Covariance Analysis Method (SSUTCAM) are used for simulation. The results indicate that UTCAM and SSUTCAM are highly efficient in calculating, with a relative error of less than 6%. Therefore, it is concluded that because of their accuracy and high efficiency, UTCAM and SSUTCAM can be adequately used in orbit insertion error analysis for a space-based gravitational wave observatory. Secondly, SSUTCAM is used to study the effects of position and velocity errors on the constellation. For the case in this paper, when the position error does not exceed 300 km, and the velocity error does not exceed 4 cm/s, the constellation remains stable.

Keywords: Space-based gravitational wave observatory; Orbit insertion error; Stability of constellation; UTCAM; SSUTCAM

1. Introduction

Gravitational waves are a prediction of Einstein's general theory of relativity. Gravitational-wave detection has been at the forefront of contemporary physics and is of great significance in astronomy and physics. In 2015, Laser Interferometer Gravitational-Wave Observatory (LIGO) detected gravitational wave signals on the ground for the first time. Compared with the ground gravitational wave observatory, the space-based gravitational wave observatory is free from the limitations of ground experimental scale and noise. Thus, it is able to detect gravitational waves in medium and low frequency and has higher sensitivity (Hechler and Folkner, 2003). The space-based gravitational wave observatory can promote the development of space technology, such as high-stability formation flying technology, high-precision gravity measurement technology, inter-satellite ultra-high precision laser interferometry technology, and drag-free control technology, which is also of great significance to global gravity field measurement, autonomous navigation, resource exploration and other technologies (Danzmann (2003)).

In the 1990s, NASA and ESA launched the project Laser Interferometer Space Antenna (LISA) together, aiming to detect gravitational waves produced by black holes evolutions and binary systems consisting of black holes and neutron stars (Vitale et al., 2002). LISA is an equilateral triangle formed by three satellites, whose center is located about 20° from the Earth as measured from the

* Corresponding author at: National Space Science Center, Chinese Academy of Sciences, Beijing 100190, China; University of Chinese Academy of Sciences, Beijing 100039, China.
E-mail address: 15046084839@163.com (Z. Li).

https://doi.org/10.1016/j.asr.2020.12.025
0273-1177/

Sun. The original arm length of LISA was 5×10^6 km. In 2011, NASA announced the withdrawal of LISA due to economic reasons, and ESA shortened the arm length to 1×10^6 km (eLISA). Thus, the difficulty of constellation design is reduced. After NASA joined LISA again, now the space-based gravitational wave observatory has an arm length of 2.5×10^6 km.

TaiJi and TianQin are Chinese space-based gravitational wave observatories. Chinese Academy of Sciences put forward TaiJi project. TaiJi consists of three satellites, figuring an equilateral triangle, and aims to detect gravitational waves at low and medium frequencies. The detection frequency band of TaiJi is 0.1 mHz-1 Hz, and it determines that the arm length is 3×10^6 km. The main scientific objective of TaiJi project is to study massive black holes, such as how the intermediate mass seed black holes were formed in the early universe (Luo et al., 2018; Hu et al., 2017). Using free-floating test masses as sensors, the gravitational wave signal is converted into the distance between masses, which is also a change of the interferometer arm length.

Sun Yat-sen University put forward TianQin project. Unlike LISA and TaiJi, TianQin plans to place three spacecraft in a near-circular orbit 10^5 km from the Earth, forming an equilateral triangle. More than gravitational waves detection, TianQin also focuses on other observations such as the Earth gravity measurement. There will be two spacecraft orbiting the Earth at an altitude of 400 km aiming at mapping the global gravitational field using laser tracking between the spacecraft. (Shi et al., 2019; Wang et al., 2019; Luo et al., 2016).

A space-based gravitational wave observatory is generally required to be designed for a long lifetime. It may be influenced by orbit insertion errors, which can impact the long-term constellation behavior. As a result, mission requirements can no longer be satisfied. Therefore, it is necessary to analyze the error propagation. Currently, the analytical approach and Monte-Carlo are widely used to address this problem. Under the two-body model, the analytical approach uses the geometric relationship between sides and angles of the triangle to get the results of error propagation. However, perturbation forces evidently cannot be neglected for a space-based gravitational wave observatory. Monte-Carlo is simple in principle and applicable to all kinds of error analysis. When 95% confidence degree is selected to guarantee the random simulated sampling deviation, the approximate relationship between the sampling number N and the failure probability P is $N = 4/P\varepsilon^2$, where, ε is the relative deviation of failure probability estimation. Only when the number of samples is large enough can the accuracy of calculation be guaranteed. Monte-Carlo will involve a large amount of calculation and is time-consuming for an extended lifetime mission.

The linear covariance method is widely used to solve orbital prediction, intersection, transfer, and other problems in the linear dynamic model. It can be used to efficiently obtain the results of error propagation. The issue of nonlinear error propagation can be addressed by many methods (Luo and Yang, 2017). Among them, covariance analysis descriptive equation technique (CADET) can solve problems in a nonlinear model. The idea of CADET originates from Extended Kalman Filter (EKF), where a nonlinear function needs to be statistically linearized, while the mean value and covariance matrix of state variables need to be obtained by integral, so as to quickly and efficiently solve the problem of error propagation (Gelb and Warren, 1973). However, the CADET method needs to solve the partial derivative matrix of the propagation equation, which may be complicated. Unscented Transformation Covariance Analysis Method (UTCAM) originates from Unscented Kalman Filter (UKF), which improves the calculation accuracy of the complex dynamic model (Simon, 2006). Spherical Simplex Unscented Transformation Covariance Analysis Method (SSUTCAM) is derived from Spherical Simplex Unscented Transformation (SSUT), which makes calculation faster than UTCAM and is suitable for the orbit insertion error analysis of a space-based gravitational wave observatory (Julier and Uhlmann, 2002).

In this paper, UTCAM and SSUTCAM are compared with Monte-Carlo to verify that they can achieve accurate results in the orbit insertion error analysis of a space-based gravitational wave observatory. Furthermore, SSUTCAM is used to analyze the stability of the constellation with orbit insertion errors, and study the influence of position and velocity errors on the stability of the constellation.

2. Dynamic model of the space-based gravitational wave observatory

TaiJi project is selected as the research object in this paper. The three satellites form an approximately equilateral triangle on the heliocentric orbit 20° behind the earth as measured from the Sun, as shown in Fig. 1. J2000 heliocentric inertial coordinate system is selected as a reference.

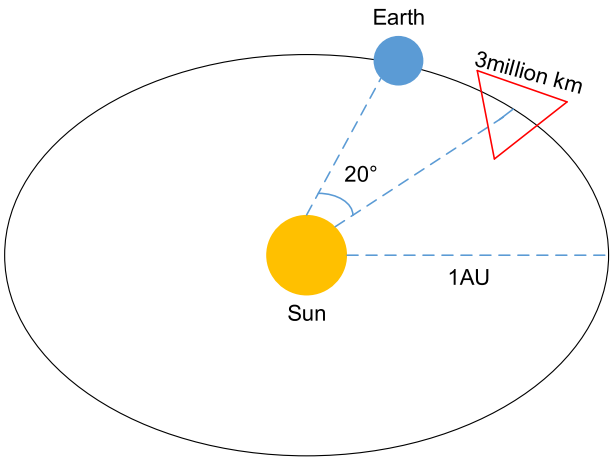

Fig. 1. Orbit of the space-based gravitational wave observatory.

Since the influences of non-conservative forces can be eliminated by a drag-free control system (Wanner et al., 2019), solar gravity and celestial perturbations need to be mainly considered for modeling (Li et al., 2008). The satellite is primarily influenced by solar gravitation and the perturbative forces of Mercury, Venus, Earth, Mars, Jupiter, Saturn, Uranus, Neptune, and the Moon. Hence, the dynamic model of the space-based gravitational wave observatory is expressed as (Dhurandhar et al., 2005).

$$\ddot{\boldsymbol{r}}_{\boldsymbol{k}} = -\mu_0 \frac{\boldsymbol{r_k}}{r_k^3} - \sum_{i=1}^{9} \mu_i \left(\frac{\boldsymbol{R_i}}{R_i^3} + \frac{\boldsymbol{r_k} - \boldsymbol{R_i}}{|r_k - R_i|^3} \right) \tag{1}$$

In Eq. (1), $\boldsymbol{r_k}$ is the position of one of the three satellites, $k = 1, 2, 3$. $\boldsymbol{R_i}$ is the position of Mercury, Venus, Earth, Mars, Jupiter, Saturn, Uranus, Neptune or the Moon, $i = 1, 2, ..., 9$, μ_0 is the constant of solar gravity and μ_i is the constant of the gravity of Mercury, Venus, Earth, Mars, Jupiter, Saturn, Uranus, Neptune, or the Moon, $i = 1, 2, ..., 9$.

The dynamic indexes of satellite formation are arm length L, breathing angle θ, arm length variation rate V, and distance between the constellation to the Earth D. These indexes can be expressed as Eqs. (2)-(5).

$$L_{ij}(t) = \| \boldsymbol{R}_{ij}(t) \| \tag{2}$$

$$\theta_i(t) = \arccos\left(\frac{\boldsymbol{R}_{ij}(t) \cdot \boldsymbol{R}_{ik}(t)}{L_{ij}(t) \cdot L_{ik}(t)}\right) \tag{3}$$

$$V_{ij}(t) = \dot{L}_{ij}(t) \tag{4}$$

$$D(t) = \| \boldsymbol{R}_e(t) - \boldsymbol{R}_c(t) \| \tag{5}$$

where $\boldsymbol{R_{ij}}(t) = \boldsymbol{R_j}(t) - \boldsymbol{R_i}(t)$ is the position vector from satellite i to satellite j, $\boldsymbol{R_e}$ is the position of the Earth, and $\boldsymbol{R_c}$ is the center of the constellation.

In TaiJi project, it is required that the arm length variation does not exceed 3.5×10^4 km, the breathing angle variation does not exceed 1°, the arm length variation rate is less than 10 m/s, and the distance between the constellation and the Earth is less than 6.5×10^7km in the lifetime. If the constellation meets the requirements above, it is considered stable. The basic experiment of TaiJi lasts for four years, and it works for the expanded experiment in the rest six years. The initial positions and velocities of the three satellites in the heliocentric J2000 coordinate system are shown in Table 1a and 1b. When the lifetime is four years, the maximum arm length is 3.014×10^6 km, the maximum breathing angle is 60.37° and the maximum arm length variation rate is 3.325 m/s in the initial constellation. When the lifetime is ten years, the maximum arm length is 3.403×10^6 km, the maximum breathing angle is 60.78° and the maximum arm length variation rate is 8.186 m/s in the initial constellation. Orbital maneuvers affect scientific experiments, so it is assumed there are no orbital maneuvers during the mission in this paper. The changes of arm length, breathing angle, and arm length variation rate are shown in Figs. 2a and 2b.

3. Application of UTCAM in the space-based gravitational wave observatory

According to Section 2, the dynamic model is nonlinear, which can be expressed as:

$$\dot{x}(t) = f(x, t) \tag{6}$$

where x_1 to x_{18} are positions and velocities of satellite 1, 2 and 3; x_{19} to x_{21} are arm lengths L of the constellation; x_{22} to x_{24} are breathing angles θ; x_{25} to x_{27} are arm length variation rates V; x_{28} is the distance to Earth D.

UTCAM draws on the idea of Unscented Transformation. For the random variable x with mean $\bar{x}$ and covariance P_x, the sampling point set is selected reasonably, and the nonlinear change is carried out for each sampling point to obtain the transformed point set $\{Y_i\}$, as well as the mean value $\bar{y}$ and covariance $\sqrt{P_y}$.

According to the mean value $\bar{x}$ and covariance P_x of the state vector x, Sigma points χ_i can be made (Simon (2006)).

$$\begin{aligned} \chi_0 &= \bar{x} \\ \chi_i &= \bar{x} + \left(\sqrt{(n+\lambda)P_x}\right)_i \qquad i = 1, \cdots, n \\ \chi_i &= \bar{x} - \left(\sqrt{(n+\lambda)P_x}\right)_i \quad i = n+1, \cdots, 2n \end{aligned} \tag{7}$$

This set of Sigma points can approximately represent the distribution of the state vector x

$$P_x = \sqrt{P_x}\sqrt{P_x}^T \tag{8}$$

$\sqrt{P_x}$ can be obtained by Cholesky decomposition.

$\left(\sqrt{(n+\lambda)P_x}\right)_i$ is the i^{th} column of the matrix, n is the dimension of x, and λ is the parameter for adjusting dispersion, controlling the distance from each point to the mean value $\bar{x}$. As shown in literature (Julier, 1995), if λ is chosen such that $n + \lambda = 3$ then the kurtosis of one state of the sigma points agrees with that of the Gaussian distribution. In this paper, n is 28, thus λ is -25.

Every Sigma point in sample points $\{\chi_i\}$ is transferred to Sigma point set after transformation $\{Y_i\}$ through nonlinear transformation. After the transformation, the Sigma

Table 1a
Initial position and velocity of three satellites in the heliocentric J2000 coordinate system (lifetime = 4 years).

	X (km)	Y (km)	Z (km)	V_x (km/s)	V_y (km/s)	V_z (km/s)
Satellite 1	−116576501.6889	85993811.7074	37270104.3844	−18.8138	−21.3165	−8.9154
Satellite 2	−115526074.8387	87735892.6966	39472663.2475	−18.9174	−20.8845	−9.2105
Satellite 3	−114337472.6307	87926599.9368	36730046.0850	−19.1108	−21.0884	−9.3118

Table 1b
Initial position and velocity of three satellites in the heliocentric J2000 coordinate system (lifetime = 10 years).

	X (km)	Y (km)	Z (km)	V_x (km/s)	V_y (km/s)	V_z (km/s)
Satellite 1	−114296153.6100	85648357.8869	35803887.9730	−19.3175	−21.4228	−9.1019
Satellite 2	−115298464.0877	85667350.2518	38606157.6353	−19.1440	−21.1820	−9.0383
Satellite 3	−113068481.9115	87490458.1497	37827255.2867	−19.4454	−20.9811	−9.4242

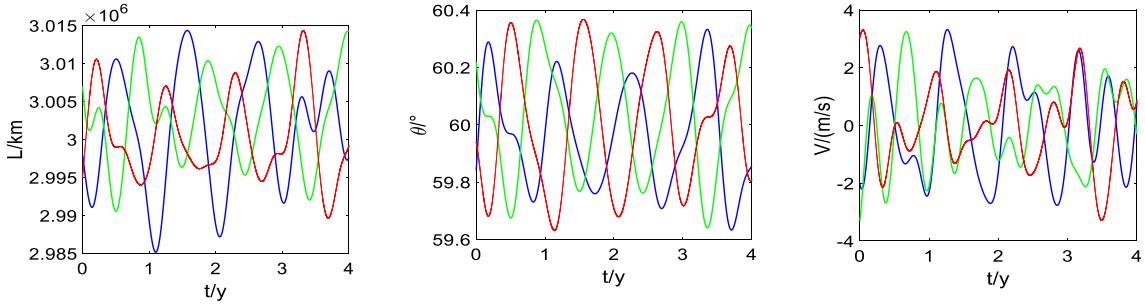

Fig. 2a. Initial constellation (lifetime = 4 years).

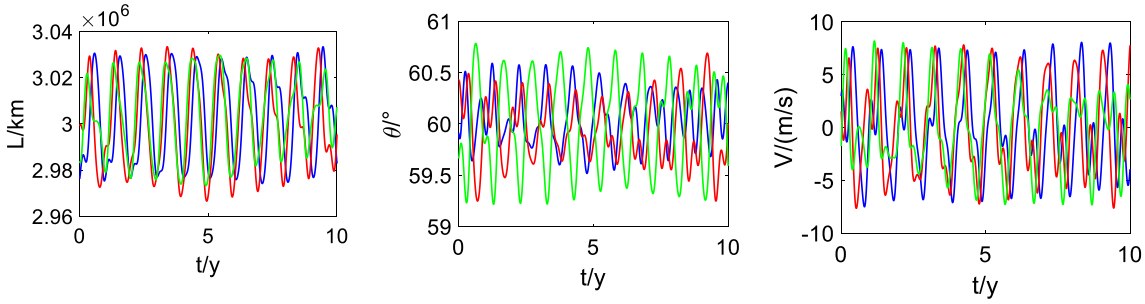

Fig. 2b. Initial constellation (lifetime = 10 years).

point set $\{Y_i\}$ is weighted to obtain the output variable $\bar{y}$ and $\sqrt{P_y}$.

$$\begin{aligned} \bar{y} &= \sum_{i=0}^{2n} W_i^{(m)} Y_i \\ P_y &= \sum_{i=0}^{2n} W_i^{(c)} (Y_i - \bar{y})(Y_i - \bar{y})^T \end{aligned} \tag{9}$$

where $W_i^{(m)}$ and $W_i^{(c)}$ are weighted coefficients for mean value $\bar{y}$ and covariance P_y, which can be set as (Simon, 2006)

$$W_i^{(m)} = W_i^{(c)} = \begin{cases} \frac{\lambda}{\lambda+n} & i = 0 \\ \frac{1}{2(\lambda+n)} & i = 1, \cdots, 2n \end{cases} \tag{10}$$

According to the equations above, the mean and covariance matrix of any time in mission lifetime can be obtained by integral. The Jacobian matrix of the dynamic model does not need to be computed. There are a total number of 28 state variables in the orbit insertion error analysis of the space-based gravitational wave observatory. UTCAM significantly reduces the calculated amount, which can apply to more complex dynamic model.

4. Application of SSUTCAM in the space-based gravitational wave observatory

The computational efficiency of UTCAM depends on the quantity of Sigma points obtained from unscented transformation. The unscented transformation in Section 3 requires $2n + 1$ symmetric points for n-dimensional state vector. It is necessary to calculate $2n + 1$ orbits for insertion error analysis of the space-based gravitational wave observatory. For an extended lifetime mission with a high-dimensional model, it takes much time.

As proved by literature (Julier and Uhlmann, 2002), at least $n + 1$ sampling points are required for n-dimensional state variables to represent the statistical characteristics of the system. Spherical Simplex Unscented Transformation (SSUT) is a method of approximating the probability distribution of variables by using $n + 1$ equally weighted sampling points distributed on the hypersphere, with the mean value of random variables as the starting point. Thus, SSUT has $n + 2$ sampling points, consisting of $n + 1$ hypersphere sampling points and an average point. It can calculate n points less than traditional unscented transformation, and has a significant advantage

in computing time. The equations of SSUT are presented below (Julier, 2003).

ε^1 is a *1*-dimensional vector with a mean value of 0 and a variance of 1. Initialize the sampling vector:

$$\begin{aligned}\varepsilon_0^1 &= [0]\\ \varepsilon_1^1 &= [-1/\sqrt{2W_1}]\\ \varepsilon_2^1 &= [1/\sqrt{2W_1}]\end{aligned} \tag{11}$$

where W_1 is the weight.

For an n-dimensional vector with a mean value of O_n and a variance of I_n(in which O_n is N-order zero matrix and I_n is N-order identity matrix), SSUT transformation is extended for n dimension according to the following equations:

$$\begin{cases}\varepsilon_{i=0}^n = \begin{bmatrix}\varepsilon_0^{n-1}\\ 0\end{bmatrix}\\ \varepsilon_{i=1,2,\cdots,n}^n = \begin{bmatrix}\varepsilon_i^{n-1}\\ -1/\sqrt{n(n+1)W_n}\end{bmatrix}\\ \varepsilon_{i=n+1}^n = \begin{bmatrix}O^{n-1}\\ n/\sqrt{n(n+1)W_n}\end{bmatrix}\end{cases} \tag{12}$$

To represent the sampling algorithm of n-dimensional vectors more intuitively, the equation is written into the matrix. The matrix $\sum^n$ consisting of n-dimensional vector sigma points set made by $n + 2$ sampling points is expressed as (Yang (2010)):

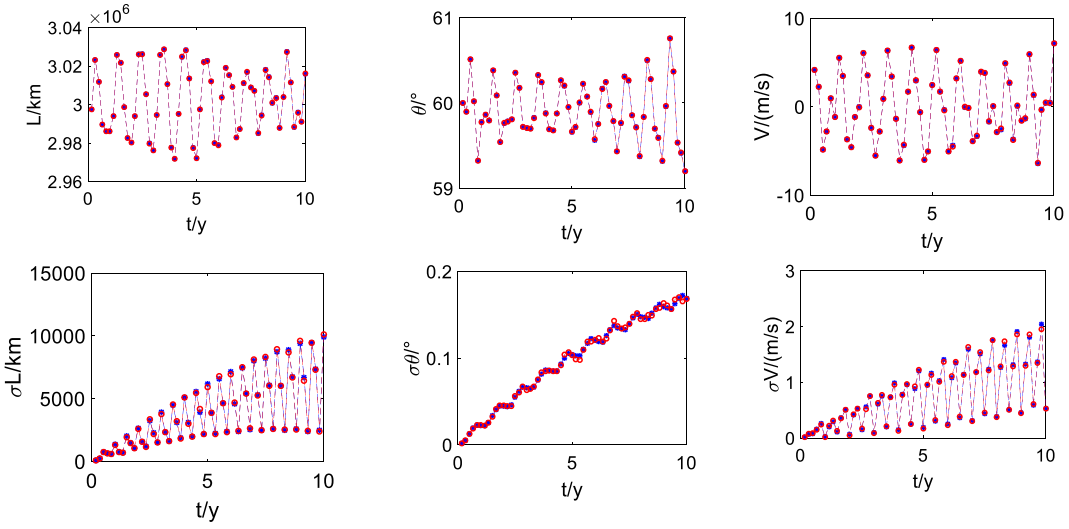

Fig. 3. Comparison diagram of UTCAM and Monte-Carlo.

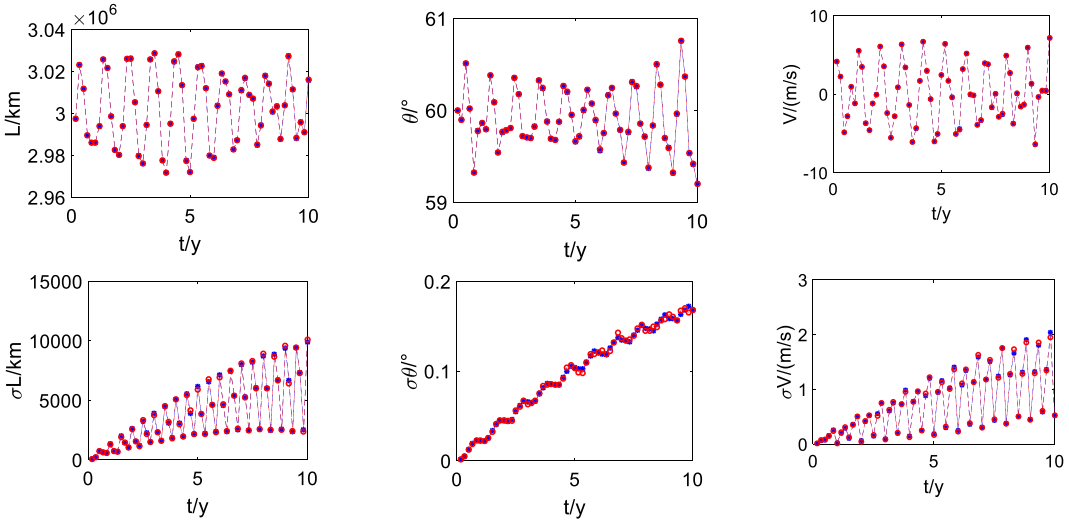

Fig. 4. Comparison diagram of SSUTCAM and Monte-Carlo.

Table 2
Comparison results of UTCAM and Monte-Carlo method.

		L_{12} (km)	L_{13} (km)	L_{23} (km)	θ_1 (°)	θ_2 (°)	θ_3 (°)	V_{12} (m/s)	V_{13} (m/s)	V_{23} (m/s)
Mean Value	MC	3016317.7921	3021446.3156	2982485.0420	59.2040	60.4837	60.3121	7.1682	−3.7070	4.3495
	UTCAM	3015963.3554	3021637.7313	2982319.1618	59.2024	60.4937	60.3039	7.1549	−3.7616	4.1919
Relative error		0.0118%	0.0063%	0.0056%	0.0027%	0.0165%	0.0136%	0.1855%	1.4729%	3.6234%
Standard Deviation	MC	10089.1313	7639.2258	2603.2693	0.1681	0.1828	0.1769	0.5253	1.4603	2.1420
	UTCAM	9897.6849	7601.5790	2456.2480	0.1688	0.1741	0.1703	0. 5299	1.4439	2.0278
Relative error		1.8976%	0.4928%	5.6476%	4.1642%	4.7593%	3.7309%	0.8757%	1.1231%	5.3315%

$$\sum^{n} = \underbrace{\begin{bmatrix} \varepsilon_0^n & \varepsilon_1^n & \varepsilon_2^n & \cdots & \varepsilon_{n+1}^n \end{bmatrix}}_{n+2} = \begin{bmatrix} 0 & \frac{-1}{\sqrt{1\times 2W_1}} & \frac{1}{\sqrt{1\times 2W_1}} & 0 & 0 & \cdots & 0 \\ 0 & \frac{-1}{\sqrt{2\times 3W_2}} & \frac{-1}{\sqrt{2\times 3W_2}} & \frac{2}{\sqrt{2\times 3W_2}} & 0 & \cdots & 0 \\ 0 & \frac{-1}{\sqrt{3\times 4W_3}} & \frac{-1}{\sqrt{3\times 4W_3}} & \frac{-1}{\sqrt{3\times 4W_3}} & \frac{3}{\sqrt{3\times 4W_3}} & \cdots & 0 \\ \vdots & \vdots & \vdots & \vdots & \vdots & \ddots & \vdots \\ 0 & \frac{-1}{\sqrt{(n-1)\times nW_{n-1}}} & \cdots & \cdots & \cdots & \cdots & 0 \\ 0 & \frac{-1}{\sqrt{n\times(n+1)W_n}} & \cdots & \cdots & \frac{-1}{\sqrt{n\times(n+1)W_n}} & \cdots & \frac{n}{\sqrt{n\times(n+1)W_n}} \end{bmatrix} \tag{13}$$

W_n is the weight corresponding to the n-dimensional vector sampling points, and it is calculated by the following equation:

$$W_i = (1 - W_0)/(n+1), i = 1, 2 \cdots n+1 \tag{14}$$

where $0 \leqslant W_0 \leqslant 1$. In this paper, $W_0 = 0.5$. If $i = 1, 2, \cdots n+1$, $W_i = W_1$. W_n can be thus replaced by W_1 in Eq. (13).

Hence, the mean value $\bar{x}$ and variance P_x of n-dimensional random vector x can be calculated by sampling points set $\sum^n$ in the SSUT method.

$$\chi_i = \bar{x} + \sqrt{P_x}\varepsilon_i^n, i = 0, 1, 2 \cdots n+1 \tag{15}$$

5. Simulations of UTCAM and SSUTCAM

Initial positions and velocities in Table 1b are selected and added with normal distribution errors. The mean value and standard deviation of the arm length L_{12}, the breathing angle θ_1, the arm length variation rate V_{12}, and the distance between the constellation and the Earth for a 10-year mission are calculated by Monte-Carlo, UTCAM, and SSUTCAM, respectively.

Figs. 3 and 4, respectively show mean value and standard deviation results obtained by UTCAM and SSUTCAM, and these results are compared with those obtained by Monte-Carlo. The red circles represent the results of Monte-Carlo for 1000 times, and the blue stars represent the results of UTCAM and SSUTCAM, respectively.

A large amount of data was generated in the simulation, so a specific point (data at the end of 10 years) was selected to be analyzed. With the orbit insertion errors, the mean values and standard deviations of UTCAM are shown in Table 2, while those of SSUTCAM are shown in Table 3.

In Table 2, the relative error of the mean value of arm length is no more than 0.0118%, and that of standard deviation is no more than 5.6476%. The relative error of the mean value of breathing angle is no more than 0.0165%, and that of standard deviation is no more than 4.7593%. The relative error of the mean value of the arm length variation rate is no more than 3.6234%, and that of standard deviation is no more than 5.3315%. It shows that UTCAM is accurate and useful for orbit insertion error analysis of the space-based gravitational wave observatory.

In Table 3, the relative error of the mean value of arm length is no more than 0.0118%, and that of standard devi-

Table 3
Comparison results of SSUTCAM and Monte-Carlo method.

		L_{12} (km)	L_{13} (km)	L_{23} (km)	θ_1 (°)	θ_2 (°)	θ_3 (°)	V_{12} (m/s)	V_{13} (m/s)	V_{23} (m/s)
Mean Value	MC	3016317.7921	3021446.3156	2982485.0420	59.2040	60.4837	60.3121	7.1682	−3.7070	4.3495
	SSUTCAM	3015963.3501	3021637.7306	2982319.1641	59.2024	60.4937	60.3039	7.1495	−3.7615	4.1919
Relative error		0.0118%	0.0063%	0.0056%	0.0027%	0.0165%	0.0136%	0.2609%	1.4702%	3.6234%
Standard Deviation	MC	10089.1313	7639.2258	2603.2693	0.1681	0.1828	0.1769	0.5253	1.4603	2.1420
	SSUTCAM	9897.6748	7599.3589	2448.7649	0.1684	0.1738	0.1699	0.5287	1.4443	2.0283
Relative error		1.8977%	5.2187%	5.9350%	1.7847%	4.9234%	3.9570%	0.6472%	1.0957%	5.3081%

Table 4
Effects of different errors on the constellation (T = 4 years).

		L_{12}(km)	θ_1(°)	V_{12}(m/s)
Position Errors(km)	100	9355	0.1668	1.951
	1000	93,530	1.678	19.32
Velocity Errors(cm/s)	1	4773	0.08482	1.015
	10	47,730	0.8562	10.13

ation is no more than 5.9350%. The relative error of the mean value of breathing angle is no more than 0.0165%, and that of standard deviation is no more than 4.9234%. The relative error of the mean value of the arm length variation rate is no more than 3.6234%, and that of standard deviation is no more than 5.3081%. It shows that SSUTCAM is accurate and useful for orbit insertion error analysis of the space-based gravitational wave observatory. Taking the results of Monte-Carlo as the standard, UTCAM and SSUTCAM are proved effective.

All above simulations are performed using a computer with Inter(R) Core (TM) i7-6700 CPU at 3.40 GHz and RAM 8.00 GB. In Tables 2 and 3, UTCAM and SSUTCAM have the same error size. Computational time of UTCAM and SSUTCAM is 466 s and 243 s respectively. Since SSUTCAM is faster than UTCAM, SSUTCAM is selected to analyze orbit insertion error propagation in the following part.

6. Orbit insertion analysis of the space-based gravitational wave observatory based on SSUTCAM

Different orbit insertion errors will have a varying influence on the constellation. When Monte-Carlo is used to analyze impact of the insertion errors on the constellation, multiple sampling is required to ensure the reliability of results. The simulation environment is same as above. When the mission lifetime is ten years, 60 sampling points is made for 1000 times Monte Carlo, it takes about 35 h. UTCAM and SSUTCAM are accurate and useful for the orbit insertion analysis of the space-based gravitational wave detection. SSUTCAM has higher computation speed and can be used for error propagation analysis. The orbit insertion errors are divided into position errors and velocity errors. The influences of these two errors on constellation are analyzed as follows.

6.1. Effects of position error on the constellation

The mission lifetime is four years. Firstly, normally distributed position errors are applied to satellites 1, 2, and 3, with mean values of 0 and standard deviations of 100 km and 1000 km, respectively. The variations of the constellation are shown in Table 4, Figs. 5, and 6.

When the position errors are added to the three satellites simultaneously, it has effects on the constellation. It is

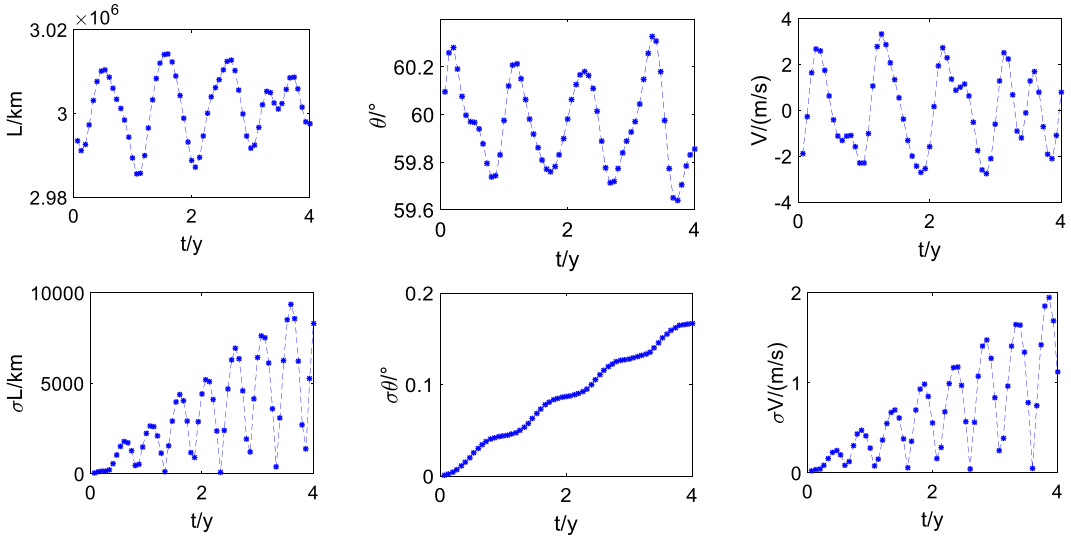

Fig. 5. Effects of 100 km position errors on the constellation.

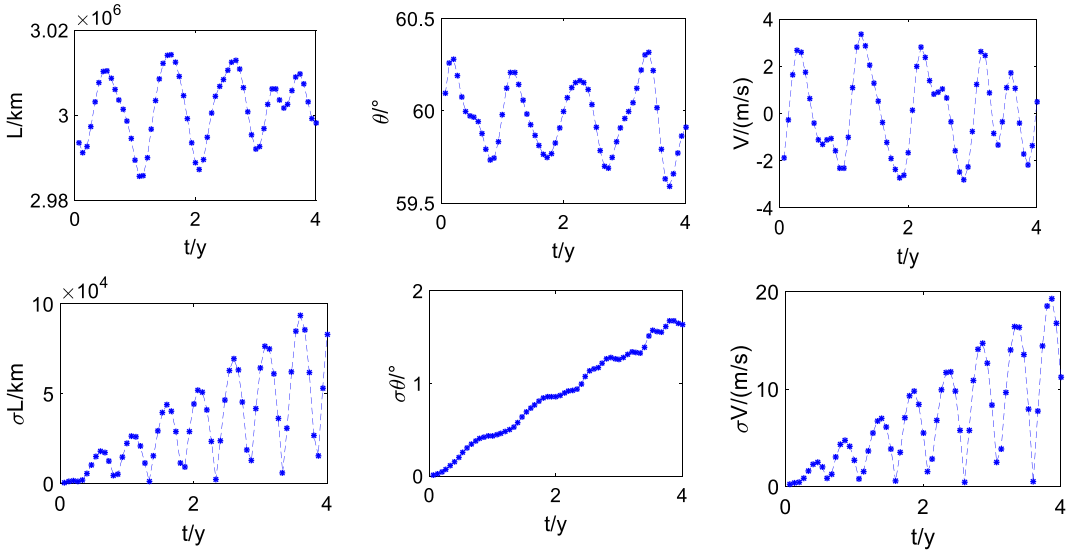

Fig. 6. Effects of 1000 km position errors on the constellation.

found that when the position error is 100 km, the constellation meets the requirements, and when the position error is 1000 km, the constellation cannot meet the requirements.

6.2. Effects of velocity error the constellation

Secondly, normally distributed velocity errors are applied to satellites 1, 2 and 3, with mean values of 0 and standard deviations of 1 cm/s and 10 cm/s, respectively. The variations of the constellation are shown in Table 4, Figs. 7, and 8.

When the velocity errors are added to the three satellites simultaneously, it has effects on the constellation. It is found that when the velocity error is 1 cm/s, the constellation meets the requirements, and when the velocity error is 10 cm/s, the constellation cannot meet the requirements.

6.3. Effects of position and velocity errors on the constellation

The position and velocity errors usually affect the constellation simultaneously, so the influence of these two errors will be analyzed as follows. When the position errors gradually increase from 100 km to 1000 km, and the velocity errors increase from 1 cm/s to 10 cm/s, the maximums of the arm length, the breathing angle and the arm length variation rate are recorded and shown in Fig. 9. In Fig. 10, when orbit insertion error is located in the blue

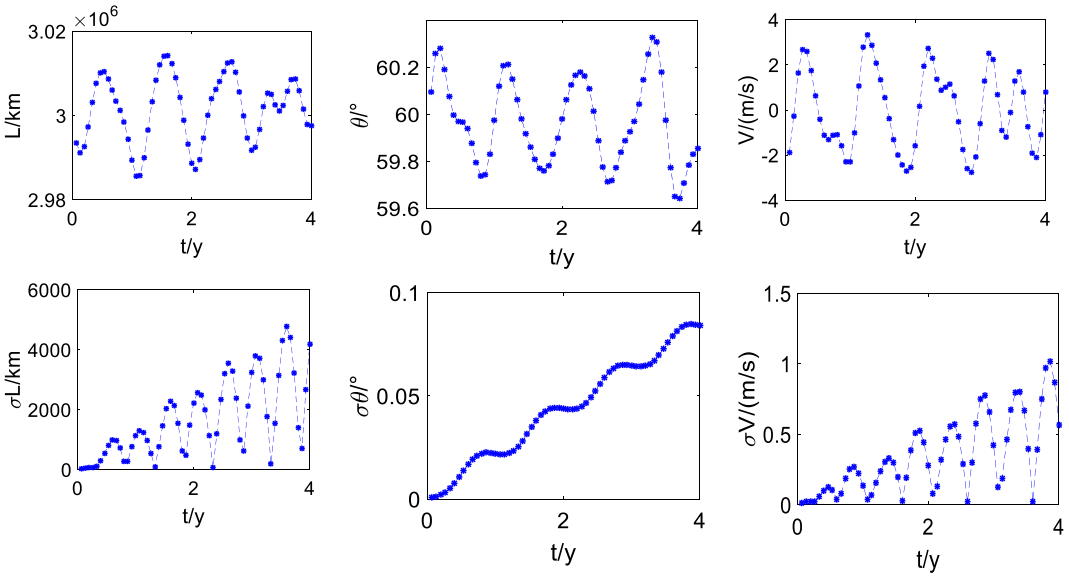

Fig. 7. Effects of 1 cm/s velocity errors on the constellation.

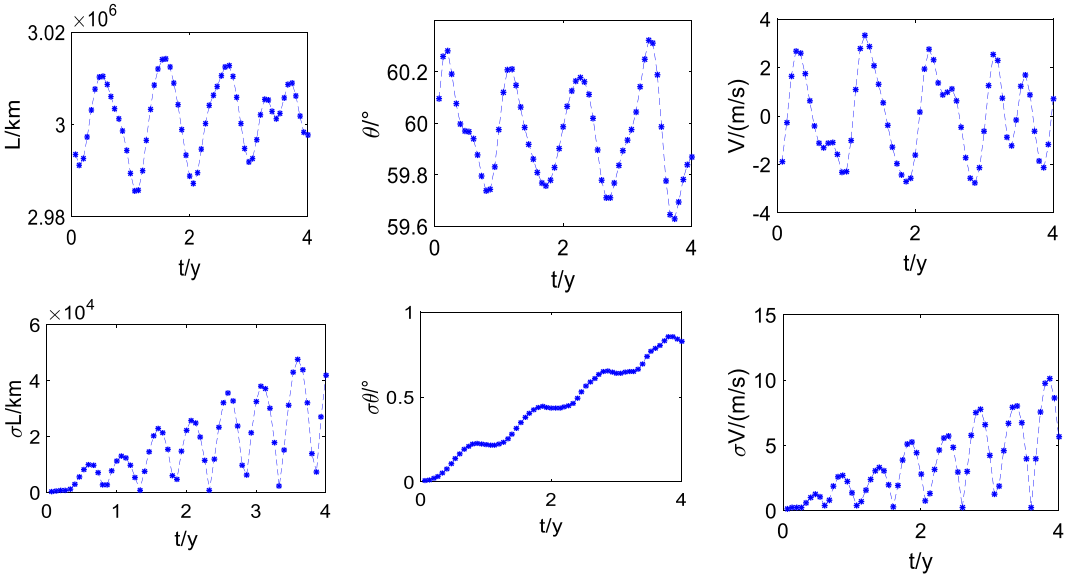

Fig. 8. Effects of 10 cm/s velocity errors on the constellation.

region, all of the arm length, the breathing angle and the arm length variation rate meet the requirements. In the green region, both the breathing angle and the arm length variation rate meet the requirements. In the yellow region, only the breathing angle meets the requirement. As the errors in position and velocity increase, the constellation enters the white region, in which none of the arm length, the breathing angle and the arm length variation rate meet the requirement. It can be concluded that the orbit insertion errors have the most significant effect on arm lengths, and they have the least effect on breathing angles. In this paper, when the position error does not exceed 300 km, and the velocity error does not exceed 4 cm/s, the constellation remains stable.

Since orbit insertion errors make the constellation diverge, orbit determination and insertion error control are necessary. Usually, an extended Kalman filter can be designed for orbit determination, while the PD controller or LQR controller can be designed for insertion error control. After orbit determination and orbit insertion error control, a high-precision constellation can be obtained.

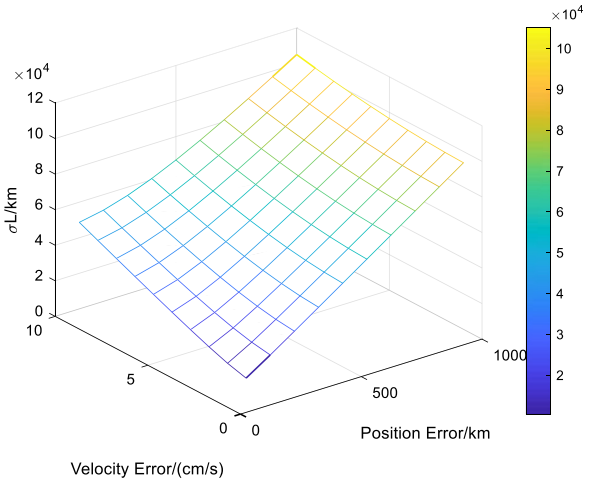

(a) Effects of position and velocity errors on the arm length

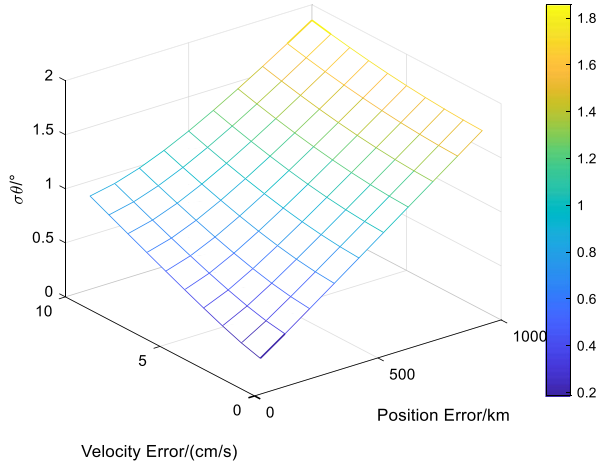

(b) Effects of position and velocity errors on the breathing angle

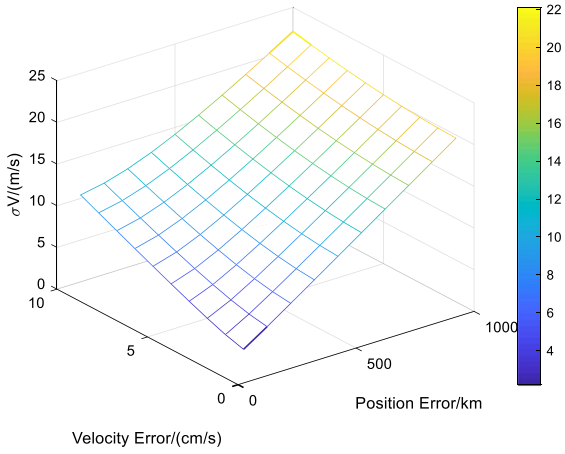

(c) Effects of position and velocity errors on the arm length variation rate

Fig. 9. Effects of position and velocity errors on the armlength, breathing angle and arm length variation rate.

7. Conclusions

Firstly, the dynamic model of the space-based gravitational wave observatory has been derived. Secondly, UTCAM and SSUTCAM for orbit insertion error propagation of the space-based gravitational wave observatory have been presented. Thirdly, UTCAM, SSUTCAM, and Monte-Carlo simulations have been carried out, and the results have been compared. Lastly, taking the constellation in this article as an example, SSUTCAM has been used to analyze the influence of the orbit insertion errors on the space-based gravitational wave observatory. Simulation results indicate that:

(1) Taking Monte-Carlo simulation results as the standard, UTCAM and SSUTCAM have relative errors of no more than 6% in ten years lifetime. UTCAM and SSUTCAM are useful in analyzing the orbit insertion error propagation;
(2) The average time of UTCAM is 466 s, and that of SSUTCAM is 243 s. These two methods are effective in rapidly predicting error propagation, which takes less time than Monte-Carlo.
(3) When there are errors in both velocity and position, the constellation remains stable if the position error does not exceed 300 km, and the velocity error does not exceed 4 cm/s in this article.

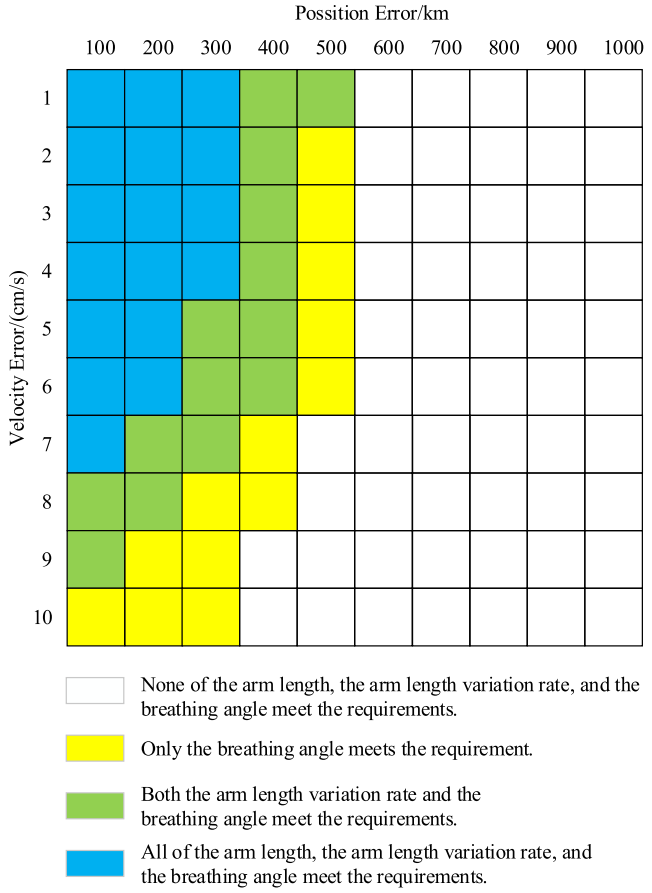

Fig. 10. Effects of position and velocity errors on the stability of the constellation.

Declaration of Competing Interest

The authors declare that they have no known competing financial interests or personal relationships that could have appeared to influence the work reported in this paper.

References

Danzmann, K., 2003. for the LISA Study Team. LISA – an ESA cornerstone mission for a gravitational wave observatory. Adv. Space Res. 32 (7), 1233–1242. https://doi.org/10.1016/s0273-1177(03)90323-1.

Dhurandhar, S.V., Nayak, K., Rajesh, K.S., Vinet, J.-Y., 2005. Fundamentals of the LISA stable flight formation. Class. Quantum Gravity 22 (3), 481–487. https://doi.org/10.1088/0264-9381/22/3/002.

Gelb, A., Warren, R.S., 1973. Direct statistical analysis of nonlinear systems: CADET[J]. AIAA J. 11 (5), 689–694.

Hechler, F., Folkner, W.M., 2003. Mission analysis for the laser interferometer space antenna (LISA) mission. Adv. Space Res. 32 (7), 1277–1282. https://doi.org/10.1016/s0273-1177(03)90332-2.

Hu, W.R., Wu, Y.L., Mechanics, I.O., et al., 2017. The Taiji Program in Space for gravitational wave physics and the nature of gravity[J]. Natl. Sci. Rev.

Julier Simon. The Spherical Simplex Unscented Transformation. Proceedings of the American Control Conference, 3, 2430-2434, 2003. https://doi.org/10.1109/ACC.2003.1243439

Julier, S.J., Uhlmann, J.K., 2002. Reduced sigma point filters for the propagation of means and covariances through nonlinear transformations[C]. Proceedings of the 2002 American Control Conference IEEE 2, 887–892.

Julier, S.J., Uhlmann, J.K., Durrant-Whyte, H.F., 1995. A new approach for filtering nonlinear systems[C]. American Control Conference IEEE.

Li Guangyu, Yi Zhaohua, Heinzel Gerhard, Rudiger Albrecht, Jennrich Oliver, Wang Li, Xia Yan, Zeng Fei, Zhao Haibin, 2008. Methods for orbit optimization for the LISA gravitational wave observatory. Int. J. Modern Phys. D, 17(07) 1021–1042. https://doi.org/10.1142/S021827180801267X.

Luo Jun, Chen Li-Sheng, Duan Hui-Zong, Gong Yun-Gui, Hu Shoucun, Ji Jianghui, Liu Qi, Mei Jianwei, Milyukov Vadim, Sazhin Mikhail, Shao Cheng-Gang, Toth Viktor T, Tu Hai-Bo, Wang Yamin, Wang Yan, Yeh Hsien-Chi, Zhan Ming-Sheng, Zhang Yonghe, Zharov Vladimir and Zhou Ze-Bing. TianQin: a space-borne gravitational wave detector. Classical and Quantum Gravity 33(3),035010,2016. https://doi.org/10.1088/0264-9381/33/3/035010.

Yazhong, L., Zhen, Y., 2017. A review of uncertainty propagation in orbital mechanics. Prog. Aerosp. Sci. 89, 23–39. https://doi.org/10.1016/j.paerosci.2016.12.002.

Ziren, L., Heshan, L., Gang, J., 2018. The recent development of interferometer prototype for Chinese gravitational wave detection pathfinder mission. Opt. Laser Technol. 105, 146–151. https://doi.org/10.1016/j.optlastec.2018.02.042.

Shi Changfu, Bao Jiahui, Wang Haitian, Zhang Jiandong, Hu Yiming, Sesana Alberto, Barausse Enrico, Mei Jianwei, and Luo Jun. Science with the TianQin observatory: preliminary results on testing the no-hair theorem with ringdown signals. Phys. Rev. D 100,044036,2019. https://doi.org/10.1103/PhysRevD.100.044036.

Simon D. Nonlinear Kalman filtering[M]// Optimal State Estimation: Kalman, H∞, and Nonlinear Approaches. John Wiley & Sons, Inc., Hoboken, New Jersey; 2006.

Vitale, S., Bender, P., Brillet, A., et al., 2002. LISA and its in-flight test precursor SMART-2[J]. Nucl. Phys. B, Proc. Suppl. 110, 209–216. https://doi.org/10.1016/s0920-5632(02)01484-6.

Wang Haitian, Jiang Zhen, Sesana Alberto, Barausse Enrico, Huang Shunjia, Wang Yifan, Feng Wenfan, Wang Yan, Hu Yiming, Mei Jianwei, and Luo Jun. Science with the TianQin observatory: Preliminary results on massive black hole binaries. Phys. Rev. D 100,043003,2019. https://doi.org/10.1103/PhysRevD.100.043003.

Gudrun, W., 2019. Space-based gravitational wave detection and how LISA Pathfinder successfully paved the way. Nat. Phys. 15, 200–202. https://doi.org/10.1038/s41567-019-0462-3.

Yang Xuerong, 2010. Study on Control Problems for the Leader-Follower Satellite Formation[D]. Graduate School of National University of Defense Technology. Changsha.